International Journal of Engineering Innovation & Research
Volume 10, Issue 3, ISSN: 2277 – 5668

Influence of Eccentric Pole Shoe on Performance of Salient Pole Electrically Excited Synchronous Motor

Ning Shan [1], Xueyi Zhang [1*], Ting Gao [1] and Ruifeng Sun [2]
[1] School of Transportation and Vehicle Engineering, Shandong University of Technology, Zibo City, Shandong Province, 255000, China.
[2] College of Forestry, Shandong Agricultural University, Taian City, Shandong Province, 271000, China.
*Corresponding author email id: zhangxueyi@sdut.edu.cn

Date of publication (dd/mm/yyyy): 05/07/2021

***Abstract* – Aiming at the problem that the power density of electrically excited synchronous generator is lower than that of permanent magnet motor, the method of pole shoe eccentricity is proposed to improve the output per--formance of motor. The air gap flux density under eccentric pole shoe is calculated analytically. The influence of eccentricity, pole arc coefficient and pole shoe thickness on motor performance is analyzed, and the important parameters are analyzed by CO simulation. The results show that proper pole shoe eccentricity can improve the sinusoidal waveform of air gap flux density, increase the output voltage of generator, and thus improve the power density of electrically excited synchronous generator.**

***Keywords* – Eccentric Pole Shoe, Salient Pole Electrically Excited Synchronous Motor, Air Gap Flux Density, Finite Element Simulation.**

I. INTRODUCTION

Synchronous motor has the advantages of high efficiency and power factor, and is widely used in electric and power generation. People pay attention to the performance of the motor, but also the demand for light weight and low cost is increasingly prominent. Compared with permanent magnet synchronous motor, electrically excited synchronous motor is widely used in high-power occasions due to its advantages of low cost, adjustable power factor and high control precision [1-4]. Aiming at the problem that the power density of electric excitation motor is lower than that of permanent magnet motor, domestic and foreign scholars at present mostly add permanent magnet to electric excitation motor to improve the power density of the motor [5-9]. However, such a hybrid excitation method increases the cost of the motor and the difficulty of control. Therefore, a salient pole electric excitation synchronous generator is taken as the sample in this paper. Based on the air-gap flux density of the motor, the influence of eccentric pole boots on the motor performance is discussed in order to improve the power density of the electrically excited synchronous motor.

II. ESTABLISHMENT OF FINITE ELEMENT MODEL OF GENERATOR

In this paper, a 3-phase 10-pole 36-slot salient pole synchronous generator with 500W power is taken as an example. The model of the generator is established by using the finite element analysis software Maxwell Ansoft. The initial model is shown in Fig. 1. The stator core and rotor core of the motor model are made of silicon steel DW310_35, and the mesh is divided by air gap stratification method to improve the simulation accuracy. The original parameters of the motor are shown in Tab. 1.

Table 1. Original parameters of generator.

Parameter	Numerical Value
Outer diameter of the stator /mm	102

Parameter	Numerical Value
Inner diameter of the stator /mm	79
Outer diameter of the rotor /mm	78
rotor poles	10
The number of stator slot	36
The number of field winding turns	100
The number of turns per slot of armature winding	22
Exciting current /A	5

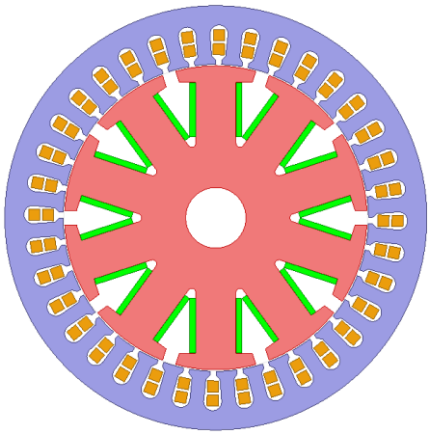

Fig. 1. Model of salient pole electrically excited synchronous generator.

III. Analytical Calculation of Air Gap Magnetic Density

When all parameters of the motor are constant except the pole boots, the distribution function $B(\theta, \alpha)$ of the air gap magnetic density corresponding to each pole of the rotor can be expressed as

$$B(\theta,\alpha)=B_r(\theta)\frac{h_m(\theta)}{h_m(\theta)+\delta_0(\theta,\alpha)} \quad (1)$$

In formula, B_r is the magnetic induction intensity generated by the excitation winding; $h_m(\theta)$ is the function of the change Angle of the radial thickness of the pole shoe along the rotation direction of the motor; $\delta(\theta, \alpha)$ is the effective air gap length; θ is the change Angle of the air gap flux density along the rotation direction of the motor; α is the relative position Angle between stator and rotor.

$h_m(\theta)$ can be expressed as

$$h_m(\theta)=R\cos\theta-L \quad (2)$$

In formula, R is the radius of rotor; L is the length of the pole body. Substituting Equation (2) into Equation (1) can be obtained

$$B(\theta,\alpha)=B_r(\theta)\frac{R\cos\theta-L}{R\cos\theta-L+\delta(\theta,\alpha)} \quad (3)$$

The center of the rotor poles were deviated, as shown in the Fig. 2.

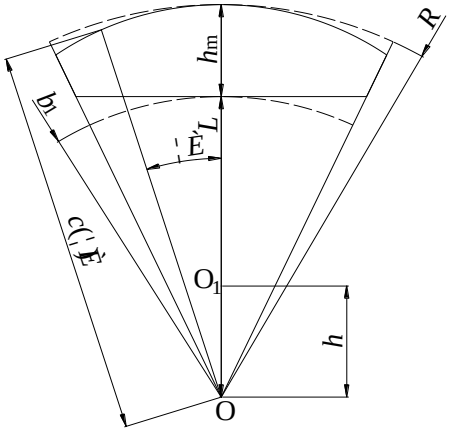

Fig. 2. The structure of the pole shoe.

The arc radius of the pole shoe surface can be obtained from Fig. 2 [10].

$$c(\theta)=h\cos\theta+\sqrt{(b_1+h_m-h)^2-(h\sin\theta)^2} \tag{4}$$

In formula, h is the eccentricity.

When the pole boots are eccentric, the effective air gap length changes accordingly. In the formula, assuming that h_m is constant, the pole shoe eccentricity can be equivalent to the air gap eccentricity, and the effective air gap length can be expressed as

$$\delta(\theta,\alpha)=\delta_0(\theta,\alpha)+R-c(\theta) \tag{5}$$

Substituting Equation (4) and (5) into Equation (3) can be obtained

$$B(\theta,\alpha)=B_r(\theta)\frac{R\cos\theta-L}{\sqrt{(b_1+h_m-h)^2-(h\sin\theta)^2}+R\cos\theta-h\cos\theta+\delta_0(\theta,\alpha)-L+R} \tag{6}$$

It can be seen from Equation 6 that, if the other parameters except the pole boots remain unchanged, the eccentricity has a great influence on the air gap magnetic density generated by the eccentric pole boots. In addition, under the premise of ensuring the reasonable structure of the motor rotor, the range of θ is determined by the pole arc coefficient, and then the range of eccentricity is determined by the pole shoe thickness together. Therefore, this paper mainly discusses the influence of the eccentricity, the thickness of the pole boots and the arc coefficient on the performance of the motor.

IV. The Influence Law of Pole Boots on Motor Performance

A. *The Influence Law of Pole Shoe Thickness on Motor Performance*

The maximum eccentricity of the pole shoe is determined by the thickness of the pole shoe to some extent. In order to comprehensively consider the influence of other factors on the motor, the pole shoe thickness is changed within the range of 2~4 mm, and the change step is 0.2 mm. The performance of the motor is simulated and analyzed. The variation of the air gap magnetic density of the generator is shown in Fig. 3, and the variation of the induced electromotive force is shown in Fig. 4.

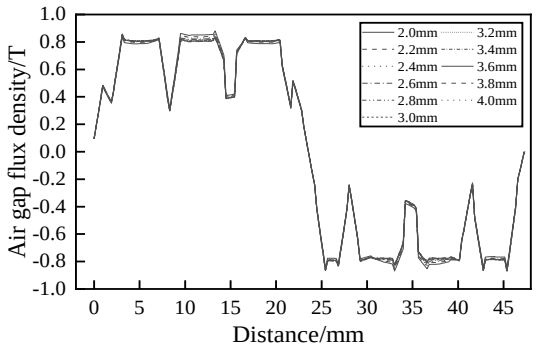

Fig. 3. Variation of air gap flux density.

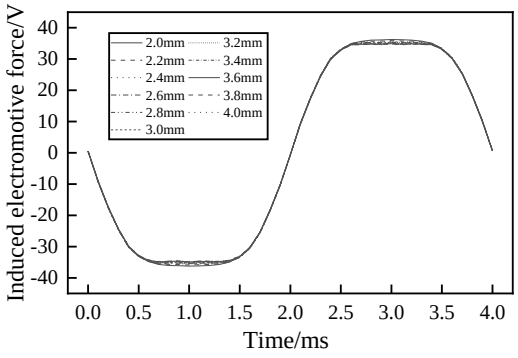

Fig. 4. Variation of induced electromotive force.

As can be seen from Fig. 3 and Fig. 4, it is obvious that the thickness of the pole boots has little influence on the motor performance, so the influence of the change of the pole boots thickness on the final result can be ignored. The change of the pole boots thickness only needs to ensure that the eccentricity is within the allowable range of the corresponding pole arc coefficient.

B. *The Influence Law of Polar Arc Coefficient on Motor Performance*

Pole arc coefficient is a coefficient describing the actual distribution of air gap magnetic field within a range of pole distance. Its size is determined by the distribution curve of magnetic field, so it is determined by the shape of excitation magnetic potential distribution curve, the uniformity of air gap and the saturation degree of magnetic circuit [11-12]. Therefore, pole arc coefficient has an important influence on motor performance. The polar arc coefficient k varies between 0.85 and 0.95, and the change step size is 0.01. The variation of the air-gap magnetic density of the generator can be obtained by simulation, as shown in Fig. 5 and Fig. 6.

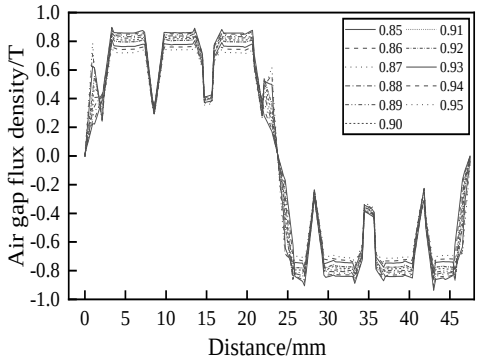

Fig. 5. Variation of air gap flux density.

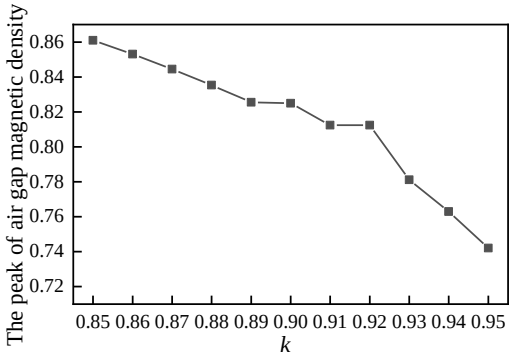

Fig. 6. Variation of peak value of air gap flux density.

As can be seen from Fig. 5, the pole-arc coefficient k affects the width of both sides of the air-gap magneto-density waveform and its peak value. The larger the pole-arc coefficient is, the wider the air-gap magneto-density waveform will be, but the peak value decreases to some extent. The smaller the polar arc coefficient, the narrower the air-gap magnetic density waveform and the higher the peak value. From this we can see the magnetic accumulation of the pole boots. As can be seen from Fig. 6, the peak value of air gap magnetic density basically decreases linearly when the polar arc coefficient is less than 0.89, fluctuates slightly between 0.89 and 0.92, and decreases rapidly when the polar arc coefficient is greater than 0.92. In addition, the changes of the induced electromotive force of the generator when the pole-arc coefficient changes are shown in Fig. 7 and Fig. 8.

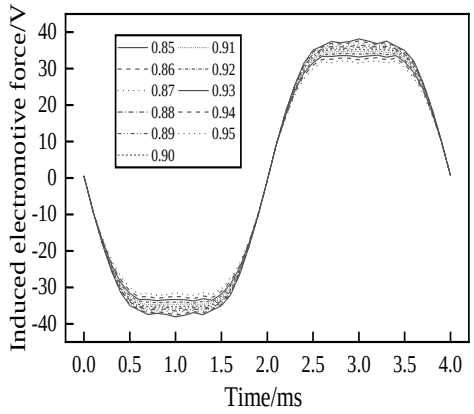

Fig. 7. Variation of induced electromotive force.

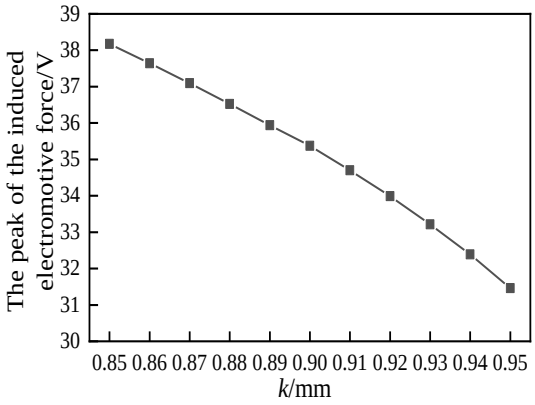

Fig. 8. Variation of peak value of induced electromotive force.

As can be seen from Fig. 7 and Fig. 8, the change of the pole-arc coefficient has little influence on the waveform shape of the induced electromotive force, and its peak value gradually decreases with the increase of the pole-arc coefficient. When *k* is less than 0.9, the decline rate of the peak value of the induced electromotive force is slightly lower than that of the peak value when *k* is greater than 0.9. In general, the polar arc coefficient should be selected in the range of small values. However, due to the limitation of magnetic saturation phenomenon of silicon steel material, too small the polar arc coefficient will lead to the magnetic field saturation of the pole boots, so a certain margin should be reserved in the selection.

C. *Influence Law of Eccentricity on Motor Performance*

The eccentricity of the pole shoe will further improve the magnetic accumulation ability of the pole shoe, so that the eccentricity *h* varies between 0~20mm, and the change step is 2mm. The variation of the generator air gap magnetic density can be obtained, as shown in Fig. 9 and Fig. 10.

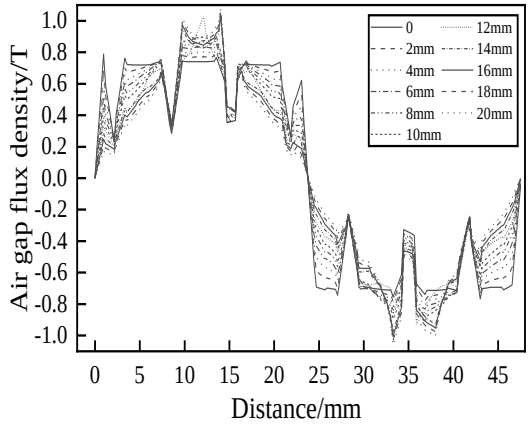

Fig. 9. Variation of air gap flux density.

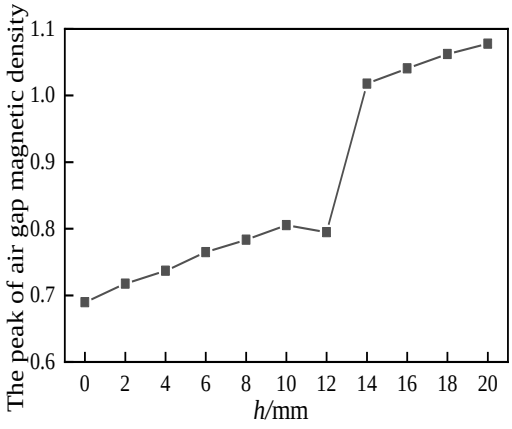

Fig. 10. Variation of peak value of air gap flux density.

As can be seen from Fig. 9, pole shoe eccentricity has a great influence on the air gap magnetic density. With the increase of eccentricity *h*, the two sides of the air gap magnetic density waveform decrease while the middle part increases, and the peak value basically shows an upward trend. However, as can be seen from Fig. 10, when *h* is less than 10mm, the peak value of air gap magnetic density increases linearly. When *h* is greater than 10mm, the peak value of the air-gap magnetic density is distorted, which decreases slightly at first and then increases sharply. When eccentricity changes, the induced electromotive force changes as shown in Fig. 11 and Fig. 12.

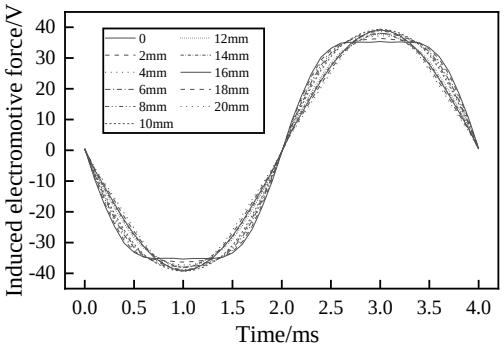

Fig. 11. Variation of induced electromotive force.

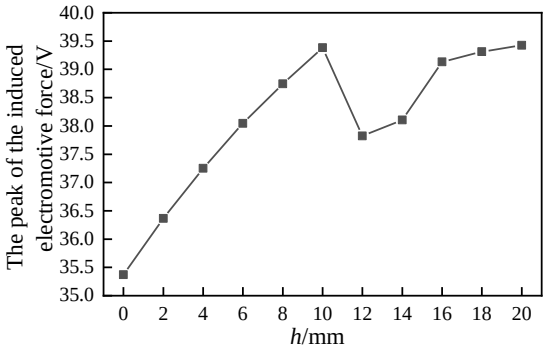

Fig.12. Variation of peak value of induced electromotive force.

As can be seen from Fig. 11, the variation of induced electromotive force corresponds to the air-gap magnetic density. With the increase of eccentricity *h*, the waveform of induced electromotive force shrinks on both sides and increases in the middle, and the sinusoidal properties are improved. As can be seen from Fig. 12, when *h* is less than 10mm, the peak value of induced electromotive force rises steadily; When *h* is greater than 10mm, the peak value of induced electromotive force decreases first and then increases, and the increase range is small. In addition, the amplitude of the induced electromotive force fundamental wave and the variation of waveform distortion rate due to the change of eccentricity are considered, as shown in Fig. 13.

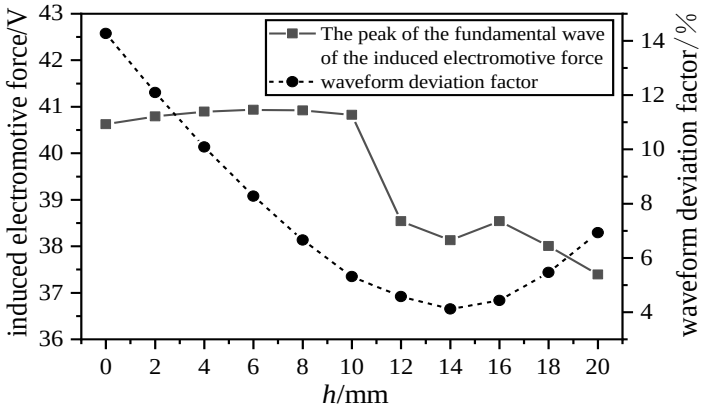

Fig. 13. Variation of fundamental amplitude and distortion rate of induced electromotive force.

As can be seen from Fig. 13, when *h* is less than 10mm, the fundamental wave amplitude of the induced electromotive force increases slowly, but the waveform distortion rate decreases significantly. When *h* is greater than 10mm, the amplitude of the induced electromotive force decreases in a fluctuating manner, and the waveform distortion decreases slowly at first and then increases gradually. Apparently eccentricity take 10 mm for pole shoe eccentric key value, when the eccentricity is greater than 10 mm motor air gap flux density and the change of the induced electromotive force is determined by the nature of the pole shoe eccentric, eccentric pole shoe by increasing the magnetic resistance at the ends of the pole shoe make central pole shoe assembled magnetic effect, but the pole shoe in the central area is lesser, magnetic ability is limited, so when the eccentricity is too large, the magnetic field intensity decreased at both ends of the pole boot due to the increase of reluctance is greater than the magnetic field intensity increased at the middle of the pole boot due to magnetic accumulation. At this time, the motor performance will change as described above.

D. *Conjoint Analysis*

The magnetic circuit of the motor is complex and changeable, and the structural parameters usually influence each other. Therefore, the joint analysis of several parameters should be considered to obtain the optimal parameter matching. The joint simulation analysis of the pole arc coefficient and the eccentricity was carried out ignoring the change of the pole shoe thickness. The pole arc coefficient varied from 0.85 to 0.95, and the change step length was 0.01. The eccentricity varies between 0 and 20mm, and the change step is 2mm. The change of the peak value of the induced electromotive force of the generator with the change of two parameters can be obtained, as shown in Fig. 14.

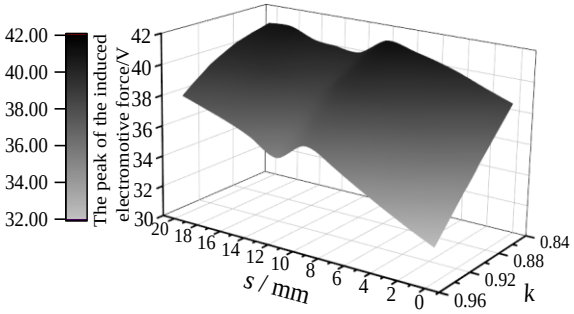

Fig. 14. The peak change of induction electromotive force under joint analysis.

As can be seen from Fig. 14, when the pole-arc coefficient is between 0.85 and 0.88, the peak value of the induced electromotive force decreases slowly, and when the eccentricity is 10mm, the peak value of the induced electromotive force is basically the maximum value. Therefore, for the generator, the eccentricity of the eccentric pole boots should be 10mm, the arc coefficient of 0.85 is appropriate.

V. Motor Performance Comparison Before and After Optimization

By analyzing the influence law of the pole shoe parameters on the motor performance and combining the simulation of several parameters, the optimal parameter matching of the eccentric pole shoe can be obtained, namely, the eccentric distance is 10mm and the pole arc coefficient is 0.85. At this time, the performance of the generator is improved compared with the prototype to a certain extent. The comparison before and after the optimization of air gap flux density is shown in Fig. 15 and Fig. 16.

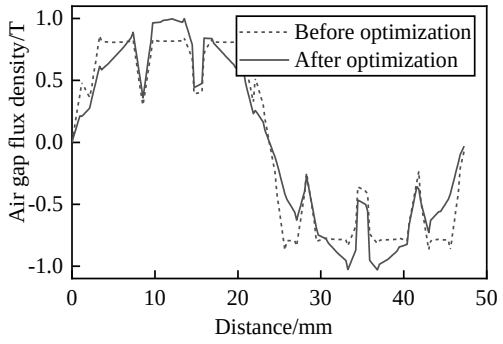

Fig. 15. Comparison of air gap flux density waveforms.

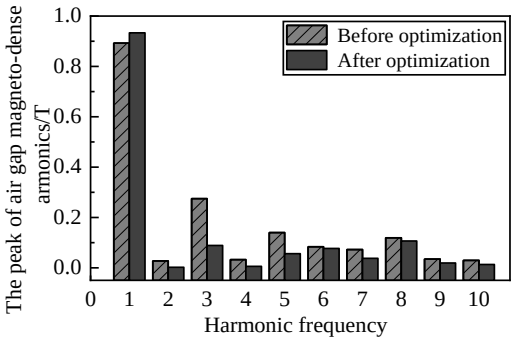

Fig. 16. Harmonic contrast of air gap flux density.

As can be seen from Fig. 15 and Fig. 16, after the pole boots are optimized, the peak value of the air gap magnetic density of the generator is significantly improved, and the fundamental wave amplitude is increased from 0.89t to 0.93t, an increase of 4.5%. The amplitude of the 2nd, 3rd, 4th, 5th and 7th harmonics was significantly reduced, and the distortion rate of the air gap magneto-dense waveform decreased from 39.6% to

18.6%. The air-gap magneto-density waveform is significantly optimized, and the output performance of the corresponding generator will also be improved. Comparison of the no-load induced electromotive force of the generator before and after optimization is shown in Fig. 17 and Fig. 18.

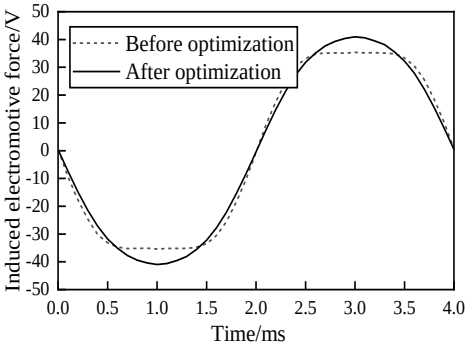

Fig. 17. Comparison of induced electromotive force.

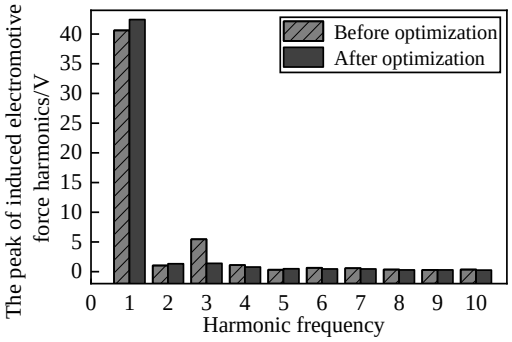

Fig. 18. Harmonic comparison of induced electromotive force.

As can be seen from Fig. 17 and Fig. 18, the no-load induced electromotive force waveform of the optimized generator is more sinusoidal, and the peak value is increased from 35.5V to 40.9V, an increase of 15.2%. The fundamental amplitude of the induced electromotive force increases from 40.6V to 42.5V, and the amplitude of the third harmonic decreases greatly, and the waveform distortion rate decreases from 14.3% to 5.4%. Under the condition of constant generator volume, the output voltage of the generator is increased through pole shoe eccentricity, and the corresponding power density will be improved.

VI. CONCLUSION

In this paper, the pole boots of salient pole excitation synchronous motor are studied in depth, and the air gap flux density waveform of the generator is improved by eccentricity of the pole boots, so as to increase the output voltage of the motor and finally improve its power density. The results show that the peak value of the induced electromotive force is increased by 15.2%, the waveform distortion rate is reduced significantly, and the performance of the generator is improved obviously when the pole boot eccentricity is 10mm and the pole arc coefficient is 0.85. As far as salient pole synchronous motor is concerned, the method of pole shoe eccentricity to optimize the air gap magnetic density is universal. This study can provide reference for the performance optimization of this type of motor.

REFERENCES

[1] Kou Baoquan, Zhao Xiaokun, Zhang Haoquan, et al. Permanent magnet synchronous motor magnetic structure and magnetic field adjusting technology review analysis [J/OL]. Proceedings of the csee: 1-18 [2021-03-30]. https://doi.org/10.13334/j.0258-8013.pcsee.202259.
[2] WU Weiliang, Yang Hemin, Yang Haiying, et al. Research on Speed Sensorless control of electrically excited synchronous motor [J]. Electric Drive, 201,51(6):38-43.
[3] Yong Bao, Zaimin Zhong, Chengyu Hu, Yijin Qin. Rotor field oriented control of resonant wireless electrically excited synchronous motor [J]. World Electric Vehicle Journal, 2019, 10(4).
[4] Jia Guanglong, Chen Zhichu, Hu Yongfeng, Li Weiye. Design and inductance parameter calculation of brushless synchronous motor with stator excitation [J]. Control & Information Technology, 2018(04): 27-31.
[5] Singh V., Kumar R., Patel SN. Non-linear vibration and instability of multi-phase composite plate subjected to non-uniform in-plane parametric excitation: semi-analytical investigation [J]. Thin-Walled Structures, 2021, 162.
[6] Yalouz S, Senjean B, Gunther J,et al. A state-averaged orbital-optimized hybrid quantum–classical algorithm for a democratic description of ground and excited states [J]. Quantum Science and Technology, 2021, 6(2): 024004.
[7] Zhang Zhuoran, Wang Dong, Hua Wei. Review and prospect of structure principle, design and operation control technology of hybrid excitation motor [J]. Proceedings of the CSEE, 2020, 40(24): 7834-7850, 8221.
[8] Zhao Guoxin, Zhang Yu, G.E. Hongyan, et al. Research on analytical calculation method of air gap magnetic density for eccentric poles permanent magnet motor [J]. Electric Machines and Control, 2020, 24(6): 24-32.
[9] Zhang Zhuoran, Wang Dong, Hua Wei. Review and prospect of structure principle, design and operation control technology of hybrid excitation motor. Proceedings of the CSEE, 2020, 40(24): 7834-7850+8221.

[10] Gong Hailong, Zhang Yanzhu, Wang Liang, Zhao Yuji, Hu Lijie, Zhang Chunli. Research on rotor pole matching of parallel rotor hybrid excitation synchronous generator [J]. Electric Machines and Control, 2020, 24(02): 128-137.
[11] Xing Zezhi, Wang Xiuhe, Zhao Wenliang. Cogging torque reduction based on segmented skewing magnetic poles with different combinations of pole-arc coefficients in surface-mounted permanent magnet synchronous motors [J]. IET Electric Power applications, 2021, 15(2): 200-213.
[12] Chen Ke, Yang Qifei, Zhou Huifang. Selection of polar Arc coefficient of permanent magnet synchronous motor [J]. Electro technical Engineering, 2020(11): 43-44, 50.

AUTHOR'S PROFILE

First Author
Ning Shan, Master in reading, Male, School of transportation and vehicle engineering, Shandong University of Technology, Shandong, Zibo, 255000, China. email id: 847024708@qq.com

Second Author
Xueyi Zhang, Doctor of Engineering, Male, Professor, School of transportation and vehicle engineering, Shandong University of Technology, China, Shandong, Zibo, 255000 (Correspondence author).

Third Author
Ting Gao, Master in reading, Male, School of transportation and vehicle engineering, Shandong University of Technology, Shandong, Zibo, 255000, China.

Fourth Author
Ruifeng Sun, Master in reading, Female, College of Forestry, Shandong Agricultural University, Shandong, Taian, 271000, China.
email id: zhangxueyi@sdut.edu.cn